J Math Chem (2013) 51:2317–2327
DOI 10.1007/s10910-013-0240-x

ORIGINAL PAPER

Modelling carbon dioxide molecule interacting with aquaglyceroporin and aquaporin-1 channels

Hakim Al Garalleh · Ngamta Thamwattana · Barry J. Cox · James M. Hill

Received: 14 June 2013 / Accepted: 18 July 2013 / Published online: 27 July 2013

Abstract Aquaporin (AQP) is a family of membrane proteins that enable water and small individual molecules to permeate cell membranes. Examples of these protein channels are aquaglyceroporin and aquaporin-1 (AQP1). Here, we investigate the permeability of carbon dioxide (CO_2) through both aquglyceroporin and AQP1 channels and explain their selectivity mechanisms. We provide a mathematical model which determines the molecular interaction potential between carbon dioxide molecule and an AQP channel. We evaluate this interaction using two approaches, namely discrete-continuum and completed discrete approaches. Both calculations agree well and our results indicate the acceptance of (CO_2) molecule into these channels which is in good agreement with other recent studies.

Keywords Aquaporins (AQPs) · Aquaporin-1 (AQP1) · Aquaglyceroporin (GlpF) · Lennard–Jones potential · Van der Waals interaction · Carbon dioxide (CO_2)

1 Introduction

Aquaporins, a large family of intrinsic membrane proteins, facilitate the transportation of water, charged and uncharged molecules through cell membranes. These channels are found in different areas in human body, mammals, bacteria and insects [1,2]. The aquaporin family is classified into two subgroups: water and aquaglyceroporin channels. Moreover, aquglyceroporins are divided into a number of subfamilies, such

H. Al Garalleh (✉) · N. Thamwattana
Nanomechanics Group, School of Mathematics and Applied Statistics,
University of Wollongong, Wollongong, NSW 2522, Australia
e-mail: hakimqaralleh@hotmail.com

B. J. Cox · J. M. Hill
Nanomechanics Group, School of Mathematical Sciences,
University of Adelaide, Adelaide, SA 5005, Australia

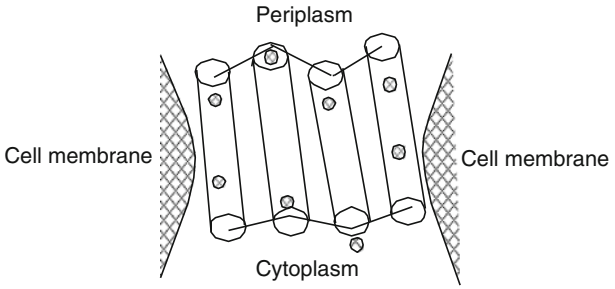

Fig. 1 Structure of functional unit of an aquaporin (either GlpF or AQP1)

as GlpF, AQP0, AQP1 and other members, which are classified depending on the compounds that are permeated through these channels, such as urea, glycerol and carbon dioxide [3,4]. Furthermore, GlpF and AQP1 channels can facilitate the transport of gases, such as NH_3 and CO_2 across membranes [5]. The structure of the GlpF facilitator has been elucidated by investigating its selectivity mechanism based on the dynamics and energetics of bio-molecules conduction [6–9]. The GlpF channel structure follows the directions of three glycerol molecules and two water molecules for each functional unit and this unit has two characteristic half-membrane-spanning repeats which are joined by quasi-two fold symmetry. For more details related to the geometrical structure of the GlpF channel we refer the reader to [6,10,11]. The structural unit of AQP1 is active as a tetramer [7] as shown in Fig. 1, and each monomer has N- and C-terminal [8] which are joined by a long loop-spanning [9,12]. Both terminals comprise three transmembrane-spanning helices [13] and the N- and the C-terminus are located on the cytoplasm side of the membrane [13,14]. For more details regarding the structure of AQP1 protein channel we refer the reader to reference [13].

Recently, the permeation of CO_2 across membranes through the selective aquaglyceroporins, GlpF and AQP1 has been reported [12,15]. Verkman et al. [16] indicate that small gases such as CO_2, NH_3 and NO transported by proteins should not be ignored. In addition, Verkman et al. [16] suggest that CO_2 molecules can pass through these channels into kidney and lung tissues. This finding is supported by Yang et al. [17], Fang et al. [18] and Wang et al. [19] who detect the transportation of CO_2 by AQP1 in lung and kidney cells. Also, the water channel AQP1 is able to transport small gas molecules, such as nitric oxide and ammonia across cell membranes [20,21].

In the present paper, we examine a flaired right cylindrical aquaporin interacting with a carbon dioxide molecule (CO_2). Various atomic interactions are modelled assuming both discrete and continuum approaches. Here, we adopt the six-twelve Lennard–Jones potential to determine the van der Waals interactions for the carbon dioxide molecule (CO_2) interacting with the GlpF and AQP1, which have chemical compositions $C_{1289}H_{2527}N_{315}O_{591}S_{11}$ and $C_{1235}H_{2468}N_{320}O_{601}S_7$, respectively [14]. We calculate the potential energy using a discrete-continuum approach by considering the carbon dioxide molecule comprising a carbon atom and a sphere of oxygen atoms. Alternatively, we find the total potential energy using a discrete model where a carbon dioxide molecule is assumed to comprise three discrete atoms; namely one carbon and two oxygen atoms.

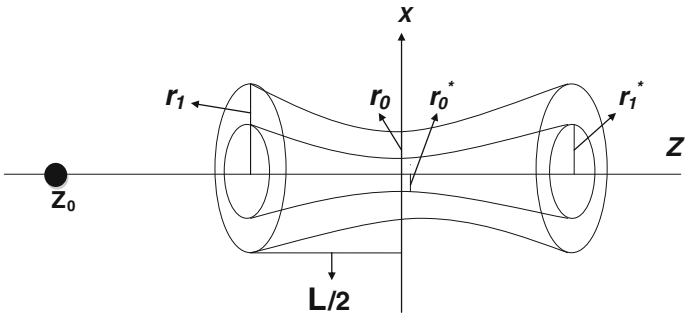

Fig. 2 Geometry of an atom interacting with a flaired right cylindrical aquaporin

In the next section, we derive an expression for the interaction potential of a carbon dioxide molecule and the GlpF and AQP1 channels. Following this we present numerical results of our model, and in the final section, we make some concluding remarks.

2 Interaction energy

2.1 Interaction between an aquaporin channel and a single atom

We begin by considering the van der Waals interaction between an aquaporin channel (GlpF and AQP1), which we assume to comprise a flaired right cylindrical shell, and an atom at an arbitrary point on the z-axis. With reference to Cartesian coordinate system (x, y, z), we assume the cylindrical shell to be located at the origin. This cylinder can be parameterized by $(r\delta\cos\theta,\ r\delta\sin\theta,\ z)$, where $\theta \in [-\pi\ ,\ \pi]$, $z \in [-L/2\ ,\ L/2]$ and $\delta \in [a\ ,\ 1]$, where $0 < a < 1$ and r is defined by the quadratic relationship

$$r = r_0 + 4(r_1 - r_0)(z/L)^2 = r_0 + \alpha z^2, \tag{1}$$

where $\alpha = 4(r_1 - r_0)/L^2$, r_0 and r_1 are the outer radii at the middle and at the opening of the aquaporin, respectively. The inner radii at the middle and at the opening of the aquaporin are given by ar_0 and ar_1 and we take $a = r_o^*/r_o \approx 0.25$. Further, we assume that a single atom is located on the z-axis at $(0, 0, z_0)$ as shown in Fig. 2.

The distance ρ between a typical volume element in the flaired cylinder and the atom at $(0, 0, z_0)$ is given by

$$\rho^2 = (r\delta\cos\theta)^2 + (r\delta\sin\theta)^2 + (z - z_0)^2 = r^2\delta^2 + (z - z_0)^2. \tag{2}$$

To find the interaction energy we adopt the Lennard–Jones potential which is given by

$$\phi(\rho) = -A\rho^{-6} + B\rho^{-12}, \tag{3}$$

where $A = 4\epsilon\sigma^6$ is the attractive constant, $B = 4\epsilon\sigma^{12}$ is the repulsive constant, ϵ is the well depth and σ is the van der Waals diamter. We also make use of the

empirical combining laws [22–24] given by $\epsilon_{12} = (\epsilon_1\epsilon_2)^{1/2}$ and $\sigma_{12} = (\sigma_1 + \sigma_2)/2$ to determine the well depth and van der Waals diameter for two atoms of different species. By summing all pair interactions, the total potential energy can be given by

$$V_{tot} = \sum_i \phi(\rho_i) \,, \tag{4}$$

where ϕ is the potential function given in (3). In the continuum approximation, we may replace this summation by the volume integral, where we assume a uniform atomic density throughout the volume of the aquaporin. Thus, from (4) we have

$$\begin{aligned} V_1 &= \eta_c \int_a^1 \int_{-\frac{L}{2}}^{\frac{L}{2}} \int_{-\pi}^{\pi} \phi(\rho)\, dV \\ &= \eta_c \int_a^1 \int_{-\frac{L}{2}}^{\frac{L}{2}} \int_{-\pi}^{\pi} r^2\delta(-A\rho^{-6} + B\rho^{-12})\, d\delta\, dz\, d\theta \,, \end{aligned} \tag{5}$$

where η_c represents the atomic density per unit volume and dV represents the volume element of the cylindrical aquaporin given by $dV = r^2\delta\ d\delta\ dz\ d\theta$. For detailed analytical evaluation of (5), we refer the reader to [25].

2.2 Interaction between an aquaporin channel and a carbon dioxide molecule

We obtain the interaction between an aquaporin and a carbon dioxide molecule using two approaches. First, we use a discrete-continuum approach where the carbon dioxide molecule is assumed to comprise a discrete carbon atom and the two oxygen atoms is assumed to be on a sphere of radius b (Fig. 3a). To find the interaction energy for the carbon atom, we use Eq. (5). For the oxygen atoms on the sphere (Fig. 3a), the interaction energy is given in the form [26]

$$\begin{aligned} V_2 &= \eta_s \pi b \int\int\int \left[\frac{A_O}{2} \left(\frac{1}{\rho(\rho+b)^4} - \frac{1}{\rho(\rho-b)^4} \right) \right. \\ &\quad \left. - \frac{B_O}{5} \left(\frac{1}{\rho(\rho+b)^{10}} - \frac{1}{\rho(\rho-b)^{10}} \right) \right] dV \\ &= \eta_s \pi b \int_a^1 \int_{-\frac{L}{2}}^{\frac{L}{2}} \int_{-\pi}^{\pi} \left[\frac{A_O}{2} \left(\frac{1}{\rho(\rho+b)^4} - \frac{1}{\rho(\rho-b)^4} \right) \right. \\ &\quad \left. - \frac{B_O}{5} \left(\frac{1}{\rho(\rho+b)^{10}} - \frac{1}{\rho(\rho-b)^{10}} \right) \right] r^2\delta\, d\delta\, dz\, d\theta, \end{aligned} \tag{6}$$

where η_s represents the atomic surface density of the sphere, and A_O and B_O are the attractive and repulsive constants for the sphere of oxygen atoms interacting with an

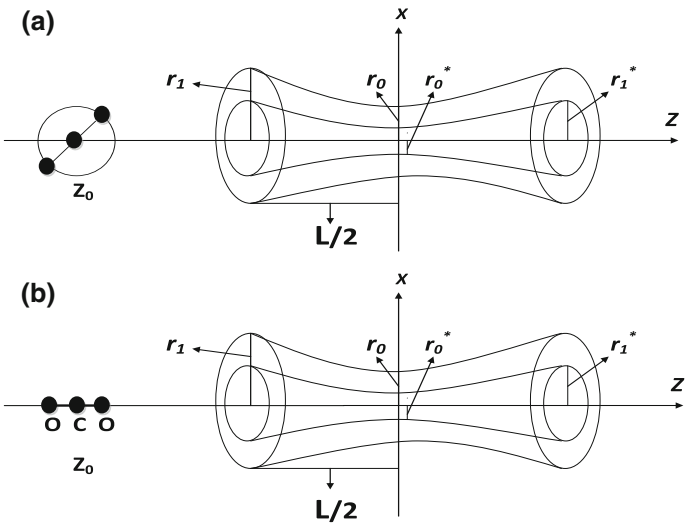

Fig. 3 Geometry of a carbon dioxide molecule centred on the z-axis interacting with flaired right cylindrical aquaporin (**a** continuum approach and **b** discrete approach)

aquaporin, respectively. Thus, by combining all interaction pairs, the total energy is given by

$$V_{tot} = V_1 + V_2. \tag{7}$$

In the second approach, we use a completed discrete method to determine the total interaction potential of a carbon dioxide molecule interacting with GlpF and AQP1 (Fig. 3b). For this case, the carbon dioxide molecule is considered as three separated atoms. The carbon atom is assumed to be located at $(0, 0, z_0)$ and the two oxygen atoms on the negative and positive sides of the carbon atom are assumed to be located at $(0, 0, z_0 - \sigma_f)$ and $(0, 0, z_0 + \sigma_f)$, respectively. Thus, the total interaction energy is given by

$$\begin{aligned} V^{tot} = \eta_c \int_{-\pi}^{\pi} \int_{a}^{1} \Bigg[& \int_{-\frac{L}{2}+\sigma_f}^{\frac{L}{2}+\sigma_f} r^2 \delta(-A_O \rho^{-6} + B_O \rho^{-12})\, dz \\ & + \int_{-\frac{L}{2}}^{\frac{L}{2}} r^2 \delta(-A_C \rho^{-6} + B_C \rho^{-12})\, dz \\ & + \int_{-\frac{L}{2}-\sigma_f}^{\frac{L}{2}-\sigma_f} r^2 \delta(-A_O \rho^{-6} + B_O \rho^{-12})\, dz \Bigg] d\delta\, d\theta\,, \end{aligned} \tag{8}$$

Table 1 Lennard–Jones constants (ϵ and σ)

Interaction	ϵ (eV $\times 10^{-2}$)	σ (Å)
C–C	0.455	3.851
C–O	0.344	3.675
O–O	0.260	3.500

Table 2 Numerical values of constants used in this model

Variable	Symbol	Value
Length of GlpF	L	28 Å
Outer radius of GlpF	r_1	15 Å
Distance between carbon and oxygen atom in CO_2	σ_f	2.055
Inner radius of GlpF	r_0	12 Å
Radius of sphere of oxygen atoms	b	1.163 Å
Volume density for GlpF	$\eta_c = N_G/V_c$	$4737/V_c = 0.3389$ atom/Å^3
Volume density for an AQP1	$\eta_c = N_Q/V_c$	$4601/V_c = 0.3292$ atom/Å^3
Surface density for CO_2 as a line	$\eta_R = 3/Length\ of\ line$	0.6374 atom/Å
Surface density for sphere of oxygen atoms	$\eta_s = 2/A_S$	0.1177 atom/Å^2
Channel wall thickness	$a = r_0^*/r_0$	0.25

where A_C and B_C are the average attractive and repulsive constants for the carbon atom and aquaporin channel, respectively. For detailed analytical evaluation of (8), we refer the reader to [25].

3 Numerical results and discussion

In this section, we evaluate the potential energy for a carbon dioxide molecule interacting with flaired right cylindrical aquaporins GlpF and AQP1 which have chemical compositions $C_{1289}H_{2527}N_{315}O_{591}S_{11}$ and $C_{1235}H_{2468}N_{320}O_{601}S_7$, respectively [14]. We provide plots of the potential energy showing the acceptance of carbon dioxide molecule using MAPLE and MATLAB softwares. The numerical values used in this model are shown in Table 1 [22,23,27–29] and Table 2 [30], where N_G and N_Q are the numbers of atoms in GlpF and AQP1 channels, respectively, V_s is the volume of the aquaporin and A_s is the surface area of the aquaporin [30]. The attractive and repulsive constants as shown in Table 3 are calculated by finding the well depth ϵ and van der Waals diameter σ for individual atoms interacting with all atoms of the aquaporin.

Figures 4–7 show the total energies arising from the interaction between a carbon dioxide molecule and two kinds of aquaporins, GlpF and AQP1. Two kinds of solutions are shown. Firstly, we refer to the infinite summation formulation given in [25] as the computational solution, and secondly a numerical evaluation of the integrals (8) utilizing the numerical integration facility of MAPLE is referred to as the numerical solution. In the calculation presented here we truncate the infinite summation in the computational solution after evaluating the first 10 terms for the five special cases as mentioned in Appendix A of [25].

Table 3 Numerical values for the attractive (A) and repulsive (B) constants

Interaction	Symbol	Value (eVÅ^6)	Symbol	Value (eVÅ$^{12} \times 10^3$)
O–O	A_{OO}	22.63	B_{OO}	41.599
O–H	A_{OH}	9.41	B_{OH}	9.972
O–S	A_{OS}	79.89	B_{OS}	228.279
O–N	A_{ON}	23.41	B_{ON}	49.283
O–C	A_{OC}	33.79	B_{OC}	83.240
H–H	A_{HH}	4.41	B_{HH}	2.548
H–S	A_{HS}	41.10	B_{HS}	70.517
H–N	A_{HN}	11.70	B_{HN}	14.383
H–C	A_{HC}	17.16	B_{HC}	52.046
C–N	A_{CN}	41.26	B_{CN}	115.661
C–S	A_{CS}	139.04	B_{CS}	522.516
S–N	A_{SN}	97.11	B_{SN}	4.772
C–C	A_{CC}	58.71	B_{CC}	191.493
N–N	A_{NN}	28.74	B_{NN}	69.083
S–S	A_{SS}	324.72	B_{SS}	1,401.426
O–GlpF	A_O	18.43	B_O	36.335
C–GlpF	A_C	32.41	B_C	99.162
O–AQP1	A_O	18.82	B_O	36.901
C–AQP1	A_C	32.45	B_C	99.031
CO_2–AQP1	A_{CO_2}	23.36	B_{CO_2}	57.611
CO_2–GlpF	A_{CO_2}	23.09	B_{CO_2}	57.277

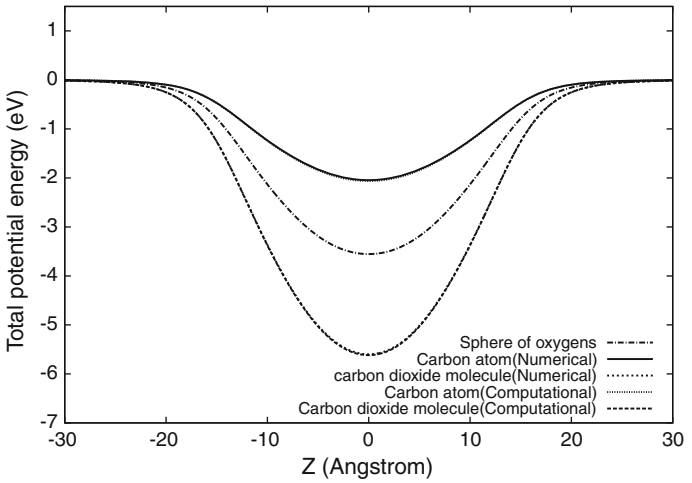

Fig. 4 Total potential energy for a carbon atom, a *sphere* of the oxygen atoms, and a carbon dioxide molecule interacting with GlpF

We evaluate and plot the potential energy arising from the interaction between the carbon atom as a specific point and oxygen atoms as a sphere interacting with the aquaporin channel GlpF as shown in Fig. 4. Both computational and numerical

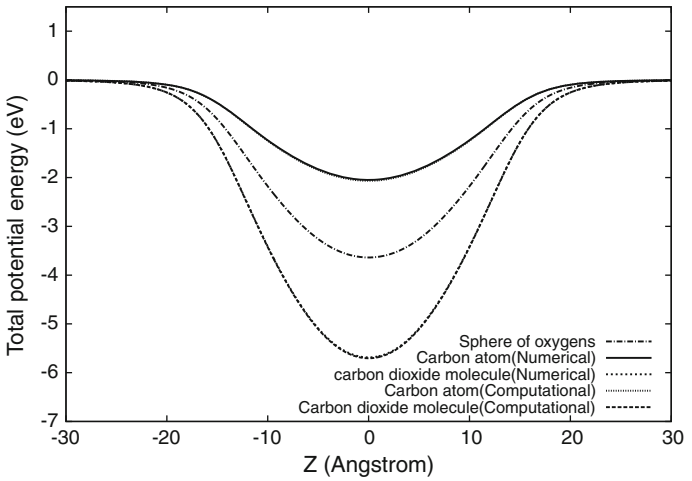

Fig. 5 Total potential energy for a carbon atom, a *sphere* of two oxygen atoms, and a carbon dioxide molecule interacting with AQP1

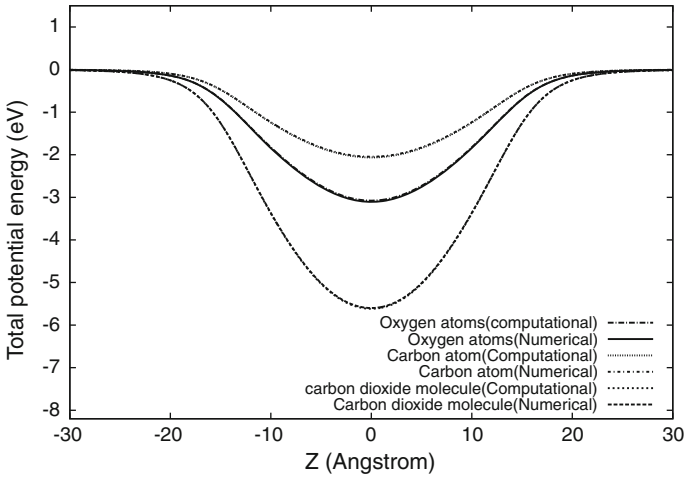

Fig. 6 Total potential energy for a carbon dioxide molecule modelled as the combination of discrete atoms interacting with GlpF

results are practically zero at $z_0 = \pm 30$ Å and beyond that it decreases gradually. Both solutions agree well and have a minimal difference in the magnitude of total energy. In our calculations, the minimum interaction energy is approximately -5.60 eV around the centre of the z-axis, thereby maximizing the van der Waals interaction. At the centre of the channel, the energy resulted from the contribution of the carbon as a discrete atom and the sphere of the two oxygen atoms are -2.05 and -3.55 eV, respectively.

In Fig. 5, we calculate the potential energy resulting from the interaction between the carbon as a single atom and the AQP1 channel. Both solutions, numerical and computational, are practically zero at $z_0 = \pm 30$ and they agree well. Next, we combine the interaction energies for the carbon atom and for the sphere of oxygen atoms. The

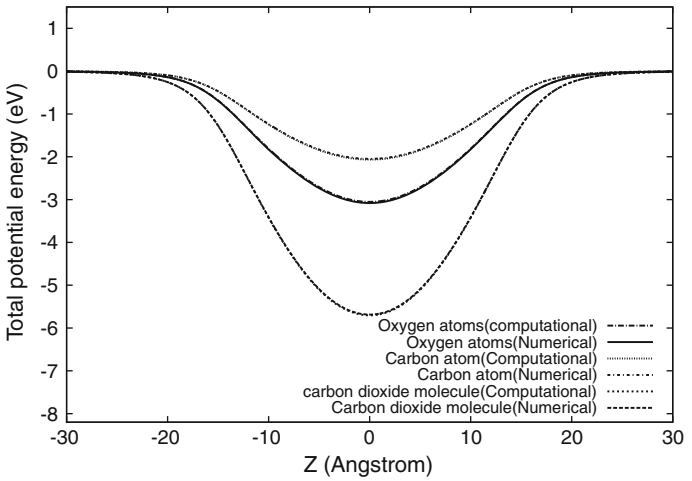

Fig. 7 Total potential energy for a carbon dioxide molecule modelled as the combination of discrete atoms interacting with AQP1

total energy profile arising from the contribution of these interactions exhibits global minimum of -5.69 eV around the centre of the AQP1 channel.

In Figs. 6 and 7, we show the total potential energy arising from the carbon dioxide molecule as three discrete atoms interacting with the GlpF and AQP1 channels, respectively. Our results indicate that the potential energies for both interactions (CO_2–GlpF and CO_2–AQp1) are practically zero at $z = \pm 30$ and the minimum potential energy for CO_2–AQP1 is -5.71 eV and that of CO_2–GlpF is approximately -5.61 eV at the centre of the z-axis (in the middle of aquaporin channel). We comment that the total potential energy around the centre is variant and depends on the kind of aquaporin channel. Our investigation demonstrates the acceptance of CO_2 molecule into the GlpF and AQP1 channels.

In conclusion, the interactions between CO_2 molecules and aquaporin channels have the global minimum energy around the centre of the z-axis, which is due to the carbon dioxide molecule being closer to the inner wall of the aquaporin and the radius of the aquaporin r being narrowest there. We find that the carbon dioxide molecule is more favourable inside the AQP1 than GlpF. Our results agree with Kruse et al. [5] and Yi et al. [19] who demonstrate the transportation of CO_2 through GlpF and AQP1 channels. Further, our results are consistent with Nakhoul et al. [20] and Holbrook and Zwieniecki [21] who show that the water channel AQP1 are able to transport small gas molecules, such as carbon dioxide, nitric oxide and ammonia through cell membrane protein.

4 Summary

We present a mathematical model which describes the acceptance of carbon dioxide molecules into protein channels. In particular, this model investigates the interaction between carbon dioxide molecule and flaired right cylindrical aquaporins, GlpF and

AQP1 channels, for which we assume a gradual change in the radius of the aquaporin channel r as a parabolic curve. We adopt the 6–12 Lennard–Jones potential to calculate the van der Waals interaction energy. Two approaches are used to model the carbon dioxide molecule, namely discrete-continuum and completed discrete approaches. Our results indicate that the aquaporin radius r plays a major role in determining the optimum energy for these interactions. The total potential energy has the global minimum energy around the centre of the cylindrical aquaporins. Consequently, our results show the acceptance of the carbon dioxide molecule inside the GlpF and AQP1 channels.

Acknowledgments The authors are grateful to the Australian Research council for support through the Discovery project scheme. They are also grateful to the provision of an UPA for HA.

References

1. G.M. Preston, T.P. Carrol, W.B. Guggino, P. Agre, Appearance of water channels in xenopus oocytes expressing red cell CHIP28 water channel. Science **256**, 385–387 (1992)
2. M.L. Zeidel, S.V. Ambudkar, B.L. Smith, P. Agre, Reconstitution of functional water channels in liposomes containing purified red cell CHIP28. Biochemistry **31**, 7436–7440 (1992)
3. C. Maurel, J. Reizer, J.I. Schroeder, M.J. Chrispeels, M.H. Saier, Functional characterization of the *Escherichiacoli* glycerol facilitator, GlpF, in xenopus oocytes. J. Biol. Chem. **269**, 11869–11872 (1994)
4. L.S. King, D. Kozono, P. Agre, From structure to disease: the evolving tale of aquaporin biology. Nat. Rev. Mol. Cell. Biol. **5**, 687–698 (2004)
5. E. Kruse, N. Uehlein, R. Kaldenhoff, The aquaporins. Genome Biol. J. **7**(2), 206–211 (2006)
6. D. Fu, A. Libson, L.J.W. Miercke, C. Weitzman, P. Nollert, J. Krucinski, R.M. Stroud, Structure of a glycerol-conducting channel and the basis for its selectivity. Science **290**, 481–486 (2000)
7. B.L. de Groot, A. Engel, H. Grubmuller, Water permeation across biological membranes: mechanism and dynamics of aquaporin-1 and GlpF. Science **294**, 2353–2357 (2001)
8. E. Tajkhorshid, P. Nollert, M.O. Jensen, L.J.W. Miercke, J. O'Connell, R.M. Stroud, K. Schulten, Control of selectivity of the squaporin water channel family by global orientational. Science **296**, 525–530 (2002)
9. M.O. Jensen, S. Park, K. Schulten, E. Tajkhorshid, Energetics of glycerol conduction through aquaglyceroporin GlpF. Proc. Natl. Acad. Sci. **99**, 6731–6736 (2002)
10. K. Murata, K. Mitsuoka, T. Hirai, T. Walz, P. Agre, J.B. Heymann, A. Engel, Y. Fujiyoshi, Structural determinants of water permeation through aquaporin-1. Nature **407**, 599–605 (2000)
11. G. Ren, V.S. Reddy, A. Cheng, A.K. Mitra, Visualization of a water-selective pore by electron crystallography in vitreous ice. Proc. Natl. Acad. Sci. **98**, 1398–1403 (2001)
12. N.L. Nakhoul, B.A. Davis, M.F. Romero, W.F. Boron, Effect of expressing the water channel aquaporin-1 on the CO_2 permeability of xenopus oocytes. Am. J. Physiol. **274**, 543–548 (1998)
13. G.M. Preston, J.S. Jung, W.B. Guggino, P. Agre, Membrane topology of aquaporin CHIP. analysis of functional epitope-scanning mutants by vectorial proteolysis. J. Biol. Chem. **269**, 1668–1673 (1994)
14. B.L. Smith, P. Agre, Erythrocyte Mr 28,000 transmembrane protein exists as a multisubunit oligomer similar to channel proteins. J. Biol. Chem. **266**, 6407–6415 (1991)
15. J.S. Hub, B.L. de Groot, Mechanism of selectivity in aquaporins and aquaglyceroporins. Proc. Natl. Acad. Sci. **105**, 1198–1203 (2008)
16. A.S. Verkman, Does aquaporin-1 pass gas? An opposing view. J. Physiol. **542**, 31 (2002)
17. B. Yang, N. Fukuda, A. Van Hoek, M.A. Matthay, T. Ma, A.S. Verkman, Carbon dioxide permeability of aquaporin-1 measured in erythrocytes and lung of aquaporin-1 null mice and in reconstituted proteoliposomes. J. Biol. Chem. **275**, 2686–2692 (2000)
18. X. Fang, B. Yang, M.A. Matthay, A.S. Verkman, Evidence against aquaporin-1-dependent CO_2 permeability in lung and kidney. J. Physiol. **542**, 63–69 (2002)
19. Y. Wang, J. Cohen, W.F. Boron, K. Schulten, E. Tajkhorshid, Exploring gas permeability of cellular membranes and membrane channels with molecular dynamics. J. Struct. Biol. **157**, 534–544 (2007)

20. N.L. Nakhoul, K.S. Hering-Smith, S.M. Abdulnour-Nakhoul, L.L. Hamm, Transport of NH_3/NH in oocytes expressing aquaporin-1. Am. J. Physiol. Renal Fluid Electrol. Physiol. **281**, 255–263 (2001)
21. N.M. Holbrook, M.A. Zwieniecki, Plant biology: water gate. Nature **425**, 361 (2003)
22. L.T. Cottrell, *The Strengths of Chemical Bonds* (Butterworths Scientific Publications, London, 1954)
23. L. Pauling, *The Nature of the Chemical Bonds* (Cornell University Press, Ithaca, NY, 1960)
24. J.O. Hirschfelder, C.F. Curtiss, R.B. Byron, *The Molecular Theory of Gases and Liquids*. Society For Industrial and Applied Mathematics. University of Winsconsin, Madison, New York (1964)
25. H. Al Garalleh, N. Thamwattana, B.J. Cox, J.M. Hill, Modelling van der waals interaction between water molecules and biological channels. J. Comput. Theor. Nanosci. **10**, 1–10 (2013)
26. B.J. Cox, N. Thamwattana, J.M. Hill, Mechanics of atoms and fullerenes in single-walled carbon nanotubes. Proc. R. Soc. A R. Soc. **463**, 461–476 (2006)
27. L.E. Sutton, *Table of interatomic distances and configuration in molecules and ions* (Chemical Society, 1965)
28. B.E. Poling, J.M. Praustmetz, J.P. O'Connell, *The Properties of Gases and Liquids* (Academic Press, Waltham, MA, 2001)
29. A.K. Rappi, C.J. Casewit, K.S. Colwell, W.M. Skid, A full periodic table force field for molecular mechanics and molecular dynamics simulations UFF. J. Am. Chem. Soc. **114**, 10024–10035 (1992)
30. D.F. Savage, P.F. Egea, C.Y. Robles, J.D. O'Conell 3rd, R.M. Stroud, Architecture and selectivity in aquaporins 2.5 Å X-ray structure of aquaporin Z. PLoS Biol. **1**, 334–340 (2003)